ANFIS BASED RECTIFIER LOAD ANALYSIS FOR ELECTRIC VEHICLE WIRELESS CHARGING SYSTEM

Dondapati Anna Mani (M.Tech) Dr. Sambasiva Rao Naraboina M.Tech, Ph.D, Hod(EEE), Professor
NRI Institute Of Technology, Pothavarappadu, Agiripalli, Krishna, Andhra Pradesh. INDIA.

annamaniabc@gmail.com nsraohodeee@gmail.com

ABSTRACT

This paper presents the analysis of rectifier load used for electric vehicle (EV) wireless charging system, as well as its applications on compensation network design and system load estimation. Firstly, a rectifier load model is established to get its equivalent input impedance, which contains both resistance and inductance components, and can be independently calculated through the parameters of the rectifier circuit. Then, a compensation network design method is proposed, based on the rectifier load analysis. Furthermore, a secondary side load estimation method and a primary side load estimation method are put forward, which adopt only measured voltages and consider the influence of the rectifier load. Finally, an EV wireless charging prototype is developed, and experimental results have proved that the rectifier equivalent load can be correctly calculated on conditions of different system load resistances, rectifier input inductances, DC voltages, and mutual-inductances. The experiments also show that rectifier load equivalent inductance will impact system performances, and the proposed methods have good accuracy and robustness in the cases of system parameter variations. Adaptive neuro-fuzzy inference systems (ANFIS) and artificial neural networks (ANN) are independently employed for the estimation process. Training data for both paradigms are extracted from analytical solution of the EV mathematical model. Comparison of the testing results signifies that ANN outperforms ANFIS in estimating the required parameters.

I. INTRODUCTION

Electric vehicle (EV) wireless charging system (WCS) has the advantages of convenience, space-saving, etc. So, it has attracted much attention. In recent years, working principle, operation characteristics, system design, and control method of

both stationary and dynamic wireless EV charging systems have been studied and applied to some demonstrations [1,2]. In applications of EV wireless charging, rectifier and output filter capacitor are needed to convert the high frequency AC to DC, in order to charge the power battery. Rectifier and the circuit after it are usually equivalent to a pure resistance load to design the system or control strategy [3,4]. A conventional way is using the coefficient 8/π 2 to make an equivalent relationship between the rectifier input impedance and the system load resistance [5,6]. However, stray parameters and non-ideal behaviors of the devices will become obvious at the high frequency range [7]. Also, rectifier input impedance can be affected by the input inductance and other parameters. So, it will bring some deviations, if only considering WCS rectifier input impedance as a pure resistance.

Actually, rectifier input impedance of EV wireless charging system contains both resistance part and inductance part [7-9]. It can be expressed as a series of an equivalent resistance and an equivalent inductance [8,9]. Although there has not been an effective method to get the equivalent load impedance of WCS rectifier, some existing researches could be helpful. Based on the on and off states [10], the rectifier and its related inductance and capacitance circuits can be described by the state space model [11], considering the stray resistances and diode forward voltage drop [12]. Then, the expressions of the related voltages and currents have been obtained in the time domain, frequency domain, or complex frequency domain [13,14], which can be used for the analysis of WCS rectifier equivalent load impedance. Besides, non-linear switching functions and circuit simulations could also be adopted to study this issue [15]. The non-linear process of rectifier load will bring some difficulties to system compensation network design. As we know, compensation networks are very important to system performances [16], and can be designed to achieve maximum efficiency, maximum power, or conjugate matching [17,18]. In most cases, a pure resistance is used to express the rectifier load [19-21]. But the operation modes of WCS rectifier load will affect the working states of compensation network [22]. So, actual equivalent input impedance of WCS rectifier load should be considered, while designing the compensation networks.

Load estimation of WCS has faced the same problem. Effects of the rectifier load could complicate the equations used for load estimation [23], and lead to the increasing of calculation and control complexity. Hence, a pure resistance load is approximately used for most of the load estimation, detection, or optimal load tracking [24-26]. Another situation is that the voltages and currents are usually both measured for load estimation, in order to calculate the impedances in the primary side [24,27]. Since the voltage and current sensors or probes have different phase delays at the high frequency range, some deviations may be introduced into the estimation process. Also, the robustness of the estimation method is very important. It can be analyzed through parameter derivation, root locus, Nyquist curve, Bode graph, or directly calculating the results on conditions of parameter variations [28-30].

Based on the previous researches, an effective method to quantitatively analyze the equivalent load of WCS rectifier is put forward in the paper firstly. The equivalent load can be independently calculated through the parameters of the rectifier circuit, and the results are basically not affected by other WCS parts. Secondly, a compensation network design method is proposed considering the equivalent impedance of the rectifier load, especially the equivalent inductance. This method will further decouple the primary and secondary side design, to achieve four system performance indicators at the same time. Thirdly, the effects of the rectifier non-linear process are taken into count to estimate the system load resistance. The proposed primary side load estimation method only adopts high frequency voltages, does not need to measure the currents, and can avoid the phase delay deviations. Also, it does not require wireless communication between the primary and secondary sides.

II. RECTIFIER LOAD ANALYSIS AND CALCULATION

Full-bridge diode rectifier is the most commonly used topology in EV wireless charging system. Also, dual-side LCC compensation networks can provide several appropriate design degrees of freedom to achieve several system performance indicators at the same time. Moreover, it can be designed to make the system resonant frequency independent of the load condition [16,22]. So we discuss the rectifier load on the basis of this kind of topology.

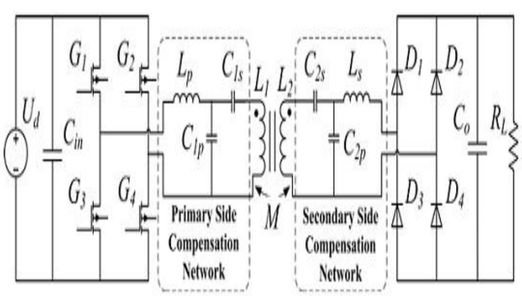

Fig.1. EV wireless charging system with full-bridge diode rectifier and dual-side LCC compensation networks.

Fig.1 shows the EV wireless charging system with full-bridge diode rectifier and dual-side LCC compensation networks; where, U_{dis} DC voltage source; the high frequency inverter is composed of G1-G4, and the full-bridge rectifier is composed ofD1-D4; the primary side compensation network consists of Lp,C1s, and C1p; the secondary side compensation network consists of Ls ,C2s, and C2p; L1andL2 are self-inductances of the transmit coil and receive coil; M is mutual-inductance between them; C_{in} and Co are system input and output filter capacitors; RLis system load resistor. It should be noticed that the WCS load is an EV power battery in the practical case, which behaves as a voltage source series with its parasitic resistance. But the power battery could be equivalent to a load resistance R_L[1,19]; the value of this equivalent resistance can be calculated by the voltage on the power battery divided by the current flowing through it. Moreover, the full-bridge rectifier, its input inductor, output filter capacitor, and the load resistor are together defined as the rectifier circuit. Although the following analysis is conducted based on the specific system, it can be extended to applications on other rectifier and compensation network topologies.

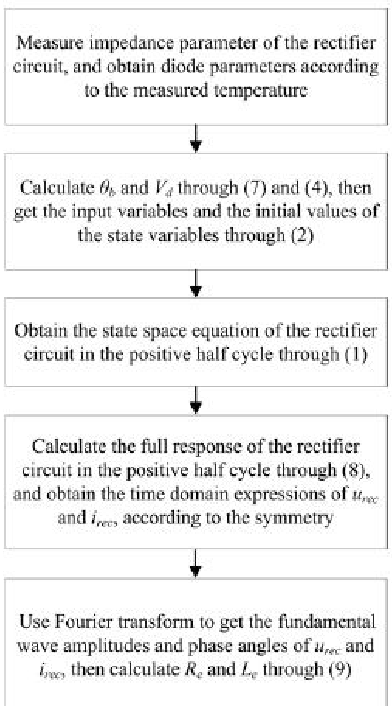

Fig. 2 Flow chart of the proposed method used to calculate the rectifier equivalent load.

Fig.3 suggests that the waveform of rectifier input current i_{rec} has some distortion, because of the effect of the rectifier input inductance. This makes the fundamental wave of i_{rec} lags behind the one of u_{rec} . So, the rectifier input impedance does not just include resistance component, but also contains a certain inductance component. Moreover, Fig.2 shows that the positive and negative half-cycles are symmetric for all the voltage and current waveforms. Hence, we just need to consider the positive half-cycle, and the negative half-cycle can be obtained from the symmetry. Fig.3 shows the equivalent circuit of the rectifier circuit in the positive half cycle, considering the stray parameters and the diode forward voltage drop; where, udio represents the diode forward voltage drop; R_{dio} is diode conduction resistance; RLs and RCoare stray resistances of Ls and Co, respectively; u_d and i_d are load voltage and current.

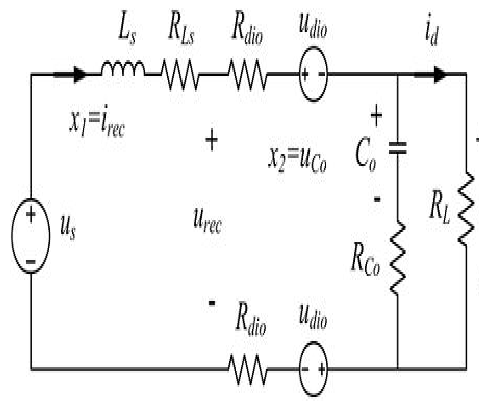

Fig. 3. Equivalent circuit of the rectifier circuit in the positive half cycle.

Based on the equivalent circuit, i_{rec} is defined as state variable x1, and the voltage on C_o is defined as state variable x2. us and u_{dio} are treated as the input variables, and u_{dis} treated as the output variable. So, state space equation of the rectifier circuit in the positive half cycle is given by (1a).

$$\begin{bmatrix} x_1' \\ x_2' \end{bmatrix} = \mathbf{A}\begin{bmatrix} x_1 \\ x_2 \end{bmatrix} + \mathbf{B}\begin{bmatrix} u_s \\ u_{dio} \end{bmatrix}, \quad y = \mathbf{C}\begin{bmatrix} x_1 \\ x_2 \end{bmatrix}. \qquad (1a)$$

Where, impedance matrixes A, B, and C are given by (1b).

$$A=\begin{bmatrix} -\frac{1}{L_s}\left(R_{Ls}+2R_{dio}+\frac{R_L R_{Co}}{R_L+R_{Co}}\right) & -\frac{1}{L_s}\left(1-\frac{R_{Co}}{R_L+R_{Co}}\right) \\ \frac{R_L}{C_o(R_L+R_{Co})} & -\frac{1}{C_o(R_L+R_{Co})} \end{bmatrix}, \quad (1b)$$

$$B=\begin{bmatrix} 1/L_s & -2/L_s \\ 0 & 0 \end{bmatrix}, \quad C=\begin{bmatrix} \frac{R_L R_{Co}}{R_L+R_{Co}} & 1-\frac{R_{Co}}{R_L+R_{Co}} \end{bmatrix}.$$

Then, the input variables and the initial values of the state variables are given by (2), according to the schematic waveforms in Fig.2; where, ω is system angle frequency; the diode forward voltage drop is treated as a constant value V_{dio}. Since only a few fluctuations exist on the voltage of C_o and the voltage drop on R_{Co} is very small, their influences can be ignored, and the initial value of x2can be approximately equivalent to a DC voltage variable V_d. Also, amplitude of us is defined as Vs, and it will be affected by WCS parameters, such as source voltage, mutual-inductance, etc. But the amplitudes of u_{rec} and i_{rec} are proportional to Vs . So, Vs can be treated as a known variable.

$$u_{s+}=V_s\sin(\omega t+\theta_b),\ u_{dio}=V_{dio},\ x_+(0)=\left[0,V_d\right]^T. \quad (2)$$

Furthermore, V_d and θ_b should be calculated to solve the state space equation. On the WCS normal working conditions, the value of V_{dio} and the voltage drops on R_{dio} and RLs are much smaller than the ones of Vs and V_d. So, the voltage on Ls is approximately equivalent to V_s sinθ-V_d, and the expression of i_{rec} can be given by (3), according to the relationship between the voltage on an inductor and the current flowing through it.

$$i_{rec}=\frac{1}{\omega L_s}\int_{\theta_b}^{\theta}(V_s\sin\theta-V_d)d\theta. \quad (3)$$

As shown in Fig.2, i_{rec}=0, when $\theta=\theta_f=\theta_b+\pi$. So, one relationship betweenV_d and θ_b can be got and given by (4).

$$V_d=(2V_s\cos\theta_b)/\pi. \quad (4)$$

Also, the DC load current I_d can be calculated by (5), which is the average value of i_d in the positive half cycle. 1

$$I_d=\frac{1}{\pi\omega L_s}\int_{\theta_b}^{\theta_b+\pi}\int_{\theta_b}^{\theta}(V_s\sin\theta-V_d)d\theta \quad (5)$$
$$=\left(V_s(2\sin\theta_b+\pi\cos\theta_b)-\pi^2V_d/2\right)/\pi\omega L_s.$$

Because I_d =V_d /RL, another relationship between V_d and θ_b can be got and given by (6).

$$V_d=V_s(2\sin\theta_b+\pi\cos\theta_b)/(\pi(\omega L_s/R_L+\pi/2)). \quad (6)$$

Based on the two relationships between V_d and θ_b, they can be obtained from (4) and (6). The expression of θ_b is given by (7), and the expression of V_d can also be got according to their relationships. Equation (7) indicates that the phase difference between u_s and u_{rec} (or i_{rec}) is mainly decided by L_s and R_L, and approximately independent of other WCS parameters. Since amplitudes of u_{rec} and i_{rec} are basically proportional to the one of us as mentioned above, we can say that the other parts of WCS have little effect on the rectifier circuit, and the rectifier load can be decoupled to analyze its equivalent input impedance. It is should be noticed that the rectifier circuit seems to be equivalent to a pure resistance RL, according to (7). However, this equivalent relationship is only suitable for (7) when calculating the phase angle θ_b, and cannot be used for any other part in the rectifier load analysis.

$$\theta_b=\arctan(\omega L_s/R_L). \quad (7)$$

After getting V_d and θ_b, full response of the rectifier circuit in the positive half cycle can be calculated by (8); where, Φ(t) is the characteristic matrix of rectifier circuit; the part before the plus sign is used for solving zero-input response, and the other part is used for solving zero-state response. On the basis of (8), time domain expressions of u_{rec} and i_{rec}

can be obtained, according to the symmetry of their waveforms.

$$x(t) = \Phi(t)x(0) + \int_0^t \Phi(\tau)\mathbf{B}u(t-\tau)\,d\tau$$
$$= e^{At}\begin{bmatrix} 0 \\ V_d \end{bmatrix} + \int_0^t e^{A\tau}\mathbf{B}\begin{bmatrix} V_s \sin(\omega(t-\tau)+\theta_b) \\ V_{dio} \end{bmatrix} d\tau. \quad (8)$$

Finally, the fundamental wave amplitudes and phase angles of u_{rec} and i_{rec} can be calculated through Fourier transform, and defined as U_{rec_fd} , I_{rec_fd} , φ_{urec_fd}, and φirec_fd . So, the equivalent input impedance of WCS rectifier load will be given by (9); where, Re and Le are series equivalent resistance and inductance of the rectifier load. Only fundamental wave is considered, because the power of the harmonics is much smaller than the one of the fundamental wave. But the harmonic input impedances can also be obtained from Fourier transform. Moreover, the calculation process suggests Re and Le will be affected by the parameters of the rectifier circuit. Hence, the robustness of this method towards parameter variation needs to be studied. But the theoretical methods, such as calculating the derivative and root locus, cannot provide a simple and clear way to analyze the robustness in this case, since it is related to some complex or non-linear operations. So, this issue will be discussed in Section V, based on the actual parameter values.

$$R_e = (U_{rec\_fd} / I_{rec\_fd})\cos(\varphi_{urec\_fd} - \varphi_{irec\_fd}),$$
$$L_e = (U_{rec\_fd} / I_{rec\_fd})\sin(\varphi_{urec\_fd} - \varphi_{irec\_fd}) / \omega. \quad (9)$$

To sum up, the above analysis suggests that the rectifier load equivalent impedance contains both resistance and inductance components. Also, the series equivalent resistance and inductance can be independently calculated through parameters of rectifier circuit, and the results are basically not affected by other WCS parameters. So, the rectifier load can be decoupled with other parts of WCS, and make system design easier.

III. COMPENSATION NETWORK DESIGN

Since the rectifier load has been decoupled with other parts of WCS, we are going to propose a compensation network design method, based on the rectifier load analysis and some existing researches [16-18]. Moreover, the proposed method will further decouple the primary and secondary side design, and make the WCS compensation network design simpler. As same as the rectifier load analysis, the dual-side LCC compensation networks are used here. The rectifier input inductance Ls should be big enough to keep the rectifier working in CCM state as mentioned above, so we will confirm it before the compensation network design. Also, the primary side compensation inductance L_p is assumed to be known, and only the four compensation capacitors are used in the design method in this section.

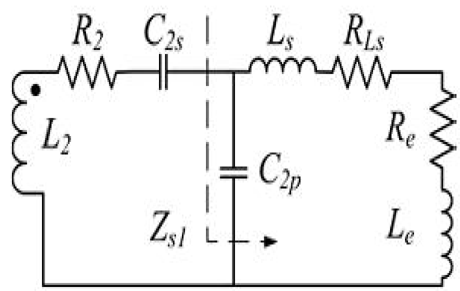

Fig.4. Equivalent circuit of the system secondary side, considering rectifier load equivalent impedance.

Firstly, the secondary side is discussed, and its equivalent circuit is shown in Fig.4; where, the series equivalent resistance Re and equivalent inductance Le are used to express the rectifier load; R2is resistance of the receive coil. As shown in Fig.4, Zs1 is defined as the impedance after the secondary side series compensation capacitor C2s, and its expression is given by (10); where, $R_e' = R_e + R_{Ls}$; $L_e' = L_e + L_s$; re(Zs1) means the real part of Zs1 ; i_m(Zs1) is the imaginary part of Zs1 .

$$re(Z_{s1}) = \frac{R_e' / (\omega^2 C_{2p}{}^2)}{R_e'^2 + (\omega L_e' - 1/(\omega C_{2p}))^2},$$
$$im(Z_{s1}) = -\frac{R_e'^2 / (\omega C_{2p}) + L_e'(\omega L_e' - 1/(\omega C_{2p}))/C_{2p}}{R_e'^2 + (\omega L_e' - 1/(\omega C_{2p}))^2}. \quad (10)$$

So, expression of the efficiency η_c can be calculated and given by (11); where, ηc is the efficiency from inverter output to rectifier load impedance; R1is resistance of the transmit coil; X_{se}=im(Zs1)+ωL2-1/(ωC2s).

$$\eta_c = \frac{re(Z_{s1})\omega^2 M^2}{(re(Z_{s1})+R_2)\omega^2 M^2 + (re(Z_{s1})+R_2)^2 R_1 + R_1 X_{se}^2}. \quad (11)$$

Equation (11) indicates that two conditions need to be met, for the sake of achieving maximum efficiency. One is X_{se} =0 to minimize the denominator of η_c . The other is the load resistance of the receive coil is equal to the optimal load resistance R_{opt}, as given by (12); where, R_{opt} are obtained from the derivation of ηc , when X_{se} =0.

$$re(Z_{s1}) = R_{opt} = \sqrt{R_2^2 + \omega^2 M^2 R_2 / R_1}. \quad (12)$$

On the basis of (10) and (12), the secondary side parallel compensation capacitor C2pcan be calculated and given by (13). According to the value of C_{2p} and the equation X_{se} =0, the secondary side series compensation capacitor C_2 scan also be solved. The above analysis suggests that the secondary side compensation capacitors can be designed independently of the primary side ones, and their design purpose is mainly to achieve maximum system efficiency.

$$C_{2p} = \frac{\omega L_e' + \sqrt{\omega^2 L_e'^2 - (R_e'^2 + \omega^2 L_e'^2)(1 - R_e'/R_{opt})}}{\omega(R_e'^2 + \omega^2 L_e'^2)}. \quad (13)$$

Then, the primary side is studied, and its equivalent circuit is shown in Fig.5; where, u_{inv} is inverter output equivalent voltage source; RLp is stray resistances of Lp; Res is the equivalent resistance of the secondary side, whenC2sand C2pare well designed, and Res= ω 2 M 2 /(Ropt+R2) .

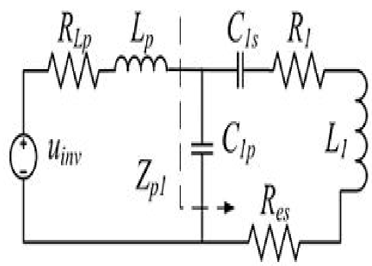

Fig. 5. Equivalent circuit of the system primary side, when the secondary side is well designed.

$$re(Z_{p1}) = \frac{(R_{es}+R_1)/(\omega^2 C_{1p}^2)}{(R_{es}+R_1)^2 + X_{pe}^2},$$
$$im(Z_{p1}) = -\frac{(R_{es}+R_1)^2 + X_{pe}(\omega L_1 - 1/(\omega C_{1s}))}{\omega C_{1p}((R_{es}+R_1)^2 + X_{pe}^2)}. \quad (14)$$

As shown in Fig.5, Zp1is defined as the impedance after the primary side compensation inductor Lp, and its expression is given by (14); where, X_{pe}=ωL1-1/(ωC1s)-1/(ωC1p); re(Zp1) means the real part of Zp1; im(Zp1) is the imaginary part of Zp1. Similar with the secondary side design, the primary side also contains two compensation capacitors with two degrees of freedom for design. So, two design targets could be added here. The first one is making the WCS output rated power. The corresponding target equation is given by (15); where, U_{inv} is the RMS value of uinv ; Poris the rated WCS output power; ηr is the rated WCS efficiency.

$$U_{inv}^2 / re(Z_{p1}) = P_{or} / \eta_r. \quad (15)$$

The second design target is keeping the input impedance of the primary side compensation network containing a certain inductance, in order to realize the soft switching of the inverter. The corresponding target equation is given by (16); where, L_{soft} is the inductance needed for inverter soft switching.

$$im(Z_{p1}) / \omega + L_p = L_{soft}. \quad (16)$$

Through simultaneously solving (15) and (16), values of the primary side compensation capacitorsC1sandC1pcan be obtained, which is not affected by the secondary side design process. Also, it should be noticed that sometimes there is no analytical solution for these equations. Numerical solution methods need to be used on this condition.

Finally, the primary and secondary side compensation networks have been decoupled for design. Also, four compensation capacitors with four degrees of freedom are designed by considering four system performance indicators, including achieving maximum efficiency, optimal load resistance, making WCS output rated power, and realizing the soft switching of the inverter. Besides, calculated values of the designed compensation capacitors require fine tuning in practice to get better results.

IV. LOAD ESTIMATION METHODS

The rectifier load analysis results can be used for system load estimation, which adopting the high frequency signals in WCS. The conventional load estimation methods are usually based on the pure resistance load, and also need the high frequency voltage and current at the same time [24,27]. The voltage and current sensors or probes will have different phase delays at the high frequency range, including the ones used in oscilloscopes and power analyzers. These different phase delays will lead to some deviations of the phase angle between the measured voltage and current, and affect the accuracy of the impedance calculation, especially when the phase angle is close to 90 °.

In order to solve this problem, we propose a load estimation method based on the secondary side high frequency voltages. The specific process is as follows: firstly, the positive zero crossings of the rectifier input voltage (urec) and the voltage before rectifier input inductor (the voltage on C2p for LCC topology) are detected, in order to obtain the positive zero crossing times. Then, define the positive zero crossing time of the voltage before rectifier input inductor as t_{ucs}, and the following positive zero crossing time of the rectifier input voltage as t_{urs}. So, the load estimation expression is given by (17), according to the relationship shown in (7). Finally, since

$$R_{L\_Sesti} = \omega L_s / \tan(\omega (t_{urs} - t_{ucs})). \qquad (17)$$

The proposed secondary side load estimation method has considered the influence of the WCS rectifier load. Also, only high frequency voltages are used in this method; no current is adopted. Hence, it can avoid the deviations introduced by different phase delays between measured voltage and current. Besides, the proposed method only detects the positive zero crossing times, but does not need the voltage amplitudes or RMS values. This will bring some simplifications to the corresponding measurements and calculations.

However, the measured signals still need to be transmitted to the primary side by wireless communication in most cases, used for system optimization or control. In order to avoid the problems brought by wireless communication, we further put forward a load estimation method based on the primary side high frequency voltages. Here, the inverter output voltage (u_{inv}) and the voltage after inverter output inductor (the voltage on C1p for LCC topology) are adopted. Define the fundamental voltage transfer function between the inverter output voltage and the voltage after inverter output inductor as G_p, and the fundamental voltage transfer function between the voltage before rectifier input inductor and the rectifier input voltage as Gs. The phase angle of G s will be θ_b as defined in Fig.2, which can be adopted for load estimation based on (7). So, we need to find a relationship between G_s and G_p, and then the measured primary side voltages can be used to calculate θ_b. To achieve this, some WCS parts can be treated as a two-port network [17,18]. Hence, the coupling coils and compensation capacitors are equivalent to a two-port network as shown in Fig.6.

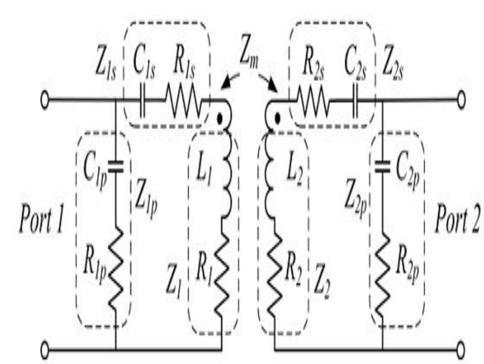

Fig. 6. Schematic of the equivalent two-port network and its parameters.

According to Fig.6, impedance parameters of the equivalent two-port network can be calculated and given by (18a).

$$\begin{aligned} Z_{11} &= Z_{1p}((Z_1+Z_{1s})(Z_2+Z_{2s}+Z_{2p})-Z_m^{\ 2})/den, \\ Z_{12} &= Z_{21} = Z_{1p}Z_{2p}Z_m/den, \\ Z_{22} &= Z_{2p}((Z_2+Z_{2s})(Z_1+Z_{1s}+Z_{1p})-Z_m^{\ 2})/den. \end{aligned} \quad (18a)$$

Where, Z_m=jωM, and the denominator denis defined by (18b).

$$den = (Z_1+Z_{1s}+Z_{1p})(Z_2+Z_{2s}+Z_{2p})-Z_m^{\ 2}. \quad (18b)$$

Then, the relationship between G_s and G_p can be got and given by (19a), based on the impedance parameters of the equivalent two-port network.

$$G_s = (n_1 G_p + n_2)/(d_1 G_p + d_2). \quad (19a)$$

Where, the coefficients n1, n2, d1, and d2are defined by (19b); where, $Zp=RL_p+j\omega Lp$; $Zs=RL_s+j\omega L_s$.

$$\begin{aligned} &n_1 = Z_{12}Z_{21}-Z_{11}Z_{22},\ d_2 = \left(Z_{11}+Z_p\right)\left(Z_{22}+Z_s\right)-Z_{12}Z_{21}, \\ &n_2 = Z_pZ_{22}+Z_{11}Z_{22}-Z_{12}Z_{21},\ d_1 = Z_{12}Z_{21}-Z_{11}\left(Z_{22}+Z_s\right). \end{aligned} \quad (19b)$$

Furthermore, the amplitudes and phase angles of the selected voltages will be measured in the primary side, and then the transfer function G_p can be obtained. Define the amplitude of G_p as Amp, and the phase angle of G_p as Php. So, θ_n, which is the phase angle of the numerator of G s , can be calculated, as well as θ_d, which is the phase angle of the denominator of G s . Their expressions are given by (20).

$$\begin{aligned} \theta_n &= \arctan\frac{Amp\cdot amn1\cdot\sin(Php+phn1)+imn2}{Amp\cdot amn1\cdot\cos(Php+phn1)+ren2}, \\ \theta_d &= \arctan\frac{Amp\cdot amd1\cdot\sin(Php+phd1)+imd2}{Amp\cdot amd1\cdot\cos(Php+phd1)+red2}. \end{aligned} \quad (20)$$

Where, amn1 and phn1 are the amplitude and phase angle of n1; amd1 and phd1 are the amplitude and phase angle of d1; ren2 and imn2 are the real and imaginary parts of n2; red2 and imd2 are the real and imaginary parts of d2; they can be calculated through (18) and (19), according to the measured values of the WCS parameters.

Finally, we can get the phase angle of Gs, and the estimated load R_{L_Pesti} can be calculated through (21). Moreover, the derivation process suggests that R_{L_Pesti} will be affected by WCS parameters, such as mutual-inductance M, compensation capacitances C1s, C_{1p},C_{2s},C_{2p}, and so on. Hence, the robustness of the estimation methods needs to be studied, when these parameters vary. But similar with the case of the rectifier equivalent load calculation method in Section II, the theoretical methods cannot provide a simple and clear way to analyze the robustness. So, this issue will be also discussed in Section V, based on the actual parameter values.

$$R_{L\_Pesti} = \omega L_s / \tan(\theta_n - \theta_d). \quad (21)$$

Developed from the above secondary side load estimation method, the proposed primary side load estimation method has also considered the influence of the rectifier load. Meanwhile, it only adopts high frequency voltages, and can avoid the phase delay deviations, too. The difference is this method needs to measure voltage amplitudes. But on the other side, it does not require wireless communication between the primary and secondary sides. So, it has some advantages in EV applications.

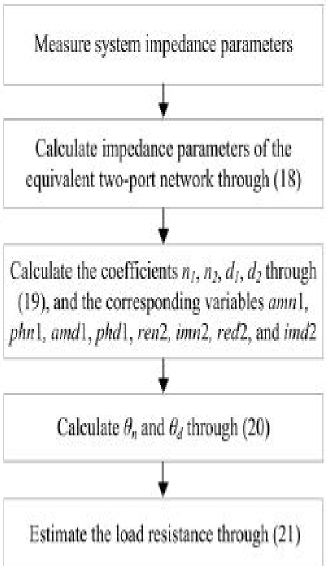

Fig. 7. Flow chart of the proposed load estimation method based on the measured primary side voltages

ANFIS Controller

In this section basics of ANFIS and development of ANFIS controller are given. ANFIS uses the neural network's ability to classify data and find patterns. It then develops a fuzzy expert system that is more transparent to the user and also less likely to produce memorization error than a neural network. ANFIS keeps the advantages of a fuzzy expert system, while removing (or at least reducing) the need for an expert. The problem with ANFIS design is that large amounts of training data require developing an accurate system. The ANFIS, first introduced by Jang in 1993, is a universal approximator and, as such, is capable of approximating any real continuous function on a compact set to any degree of accuracy. ANFIS is a method for tuning an existing rule base with a learning algorithm based on a collection of training data. This allows the rule base to adapt. As a simple example, a fuzzy inference system with two inputs x and y and one output z is assumed.

The first-order Sugeno fuzzy model,

a typical rule set with two fuzzy If–Then rules can be expressed as

Rule 1: If x is A1 and y is B1, then f1=p1x+q1y+r1

Rule 2: If x is A2 and y is B2, then f2=p2x+q2y+r2

The resulting Sugeno fuzzy reasoning system is shown here, the output z is the weighted average of the individual rules outputs and is itself a crisp value

Layer 1:

If the firing strengths of the rules are w1 and w2 , respectively, for the particular values of the inputs Ai and integral of Bi, then the output computed as weighted average,

Layer 2: .Every node in layer 2 is a fixed node, whose output is the product of all incoming signals. Wi = µAi(x) µBi(y), i=1,2

Layer 3: This layer normalizes each input with respect to the others (The I th node output is the I thinput divided the sum of all the other inputs).

Layer 4: This layer's I th node output is a linear function of the third layer's I th node output and the ANFIS input signals.

Layer 5: This layer sums all the incoming signals

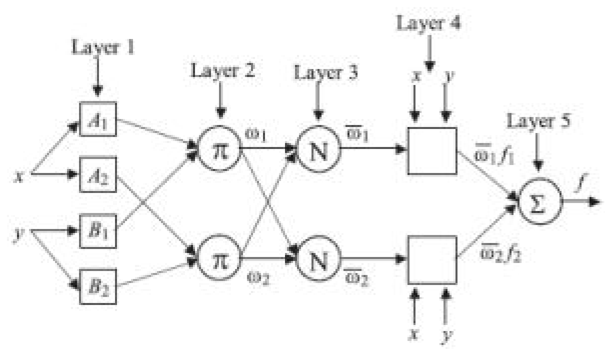

Fig:8 stracture of ANFIS

SIMULATION RESULTS

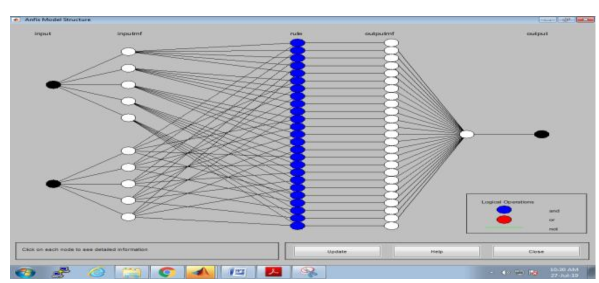

FIG9: STRACTURE OF ANFIS

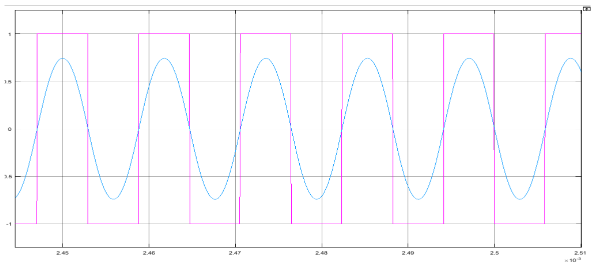

(a) Rectifier input voltage and current waveforms.

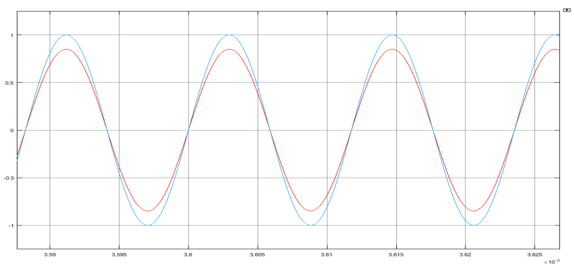

(b) Calculated fundamental waves.

Fig. 10. Experimental results of rectifier input voltage and current, as well as their fundamental waves, based on the standard parameter values

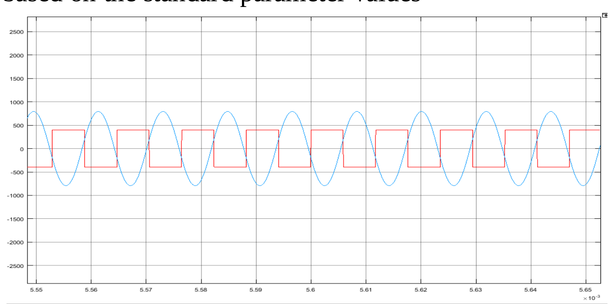

(a) Measured voltages used for secondary side load estimation

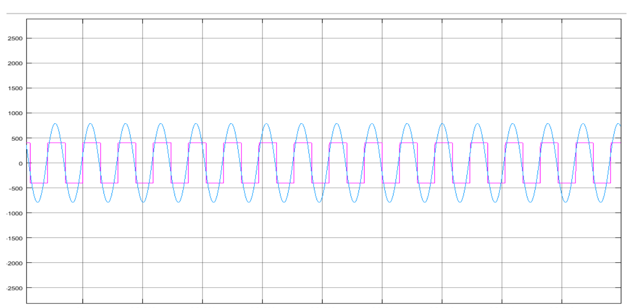

(b) Measured voltages used for primary side load estimation.

Fig. 11. Experimental results of the system voltages used for load estimations based on the standard parameter values

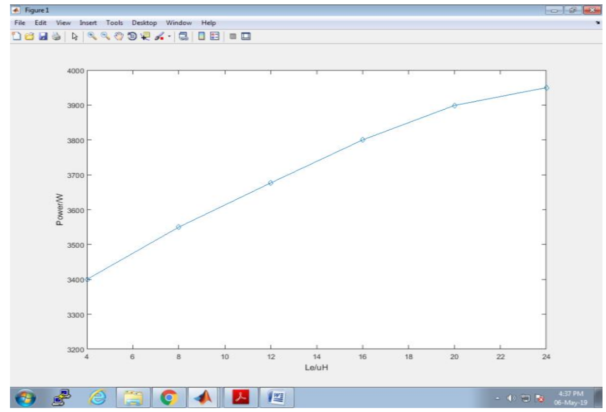

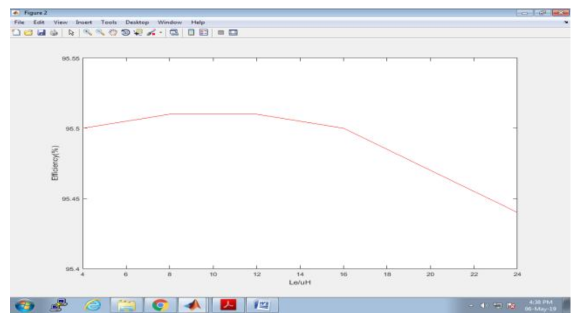

FIG: 9 Simulation results of *Le* effects on output power and efficiency.

.CONCLUSION

This paper presents a systematic analysis of the rectifier load used for EV wireless charging system. The rectifier load model has been established to calculate its equivalent input impedance, which contains both resistance and inductance components, and can be independently calculated through the parameters of the rectifier circuit. Based on the rectifier load analysis, a compensation network design method is proposed to achieve the decoupling design of the primary and secondary side compensation capacitors. Furthermore, a secondary side load estimation method and a primary side load estimation method are put forward, considering the influence of the rectifier load. They adopt only measured voltages to avoid the deviations introduced by different phase delays between measured voltage and current. Finally, the established model, the proposed rectifier load calculation method, compensation network design method, secondary and primary side load estimation methods have been verified, based on the developed EV wireless charging prototype. Although the works in this paper are conducted based on the specific system, they can be extended to more applications, such as wireless charging systems with other rectifier or compensation network topologies, etc. They will be helpful for system design and control to make EV wireless charging systems achieve stable operation and high performance.

The ANFIS method presented in this paper shows a good potential to model complex, nonlinear and multivariate problems. Considering the complexity of the relationship between the input and the output, results obtained are very accurate and encouraging. It may be noted that a trial and error procedure has to be performed for ANN model to develop the best network structure, while such a procedure is not required in developing an ANFIS model. Observations made from comparing the results are backed by the fact that results from ANN are largely dependent on architecture of the network, which is very hard to select as it is a complex and time-consuming task. Another limitation that ANN has its inadequate ability to deal with fuzzy and nonlinear data, whereas ANFIS is largely free from both of those limitations. Furthermore, computationally the ANFIS model is more easy and efficient than the ANN model. So the results suggest that the ANFIS method is superior to the ANN method.

REFERENCES

[1] S. Q. Li, and C. C. Mi, “Wireless power transfer for electric vehicle applications,” IEEE J. Emerg. Sel. Topics Power Electron., vol. 3, no. 1, pp. 4-17, Mar. 2015.

[2] Y. D. Ko, and Y. J. Jang, “The optimal system design of the online electric vehicle utilizing wireless power transmission technology,” IEEE Trans. Intell. Transp. Syst., vol. 14, no. 3, pp. 1255-1265, Sep. 2013.

[3] W. X. Zhong, and S. Y. R. Hui, “Maximum energy efficiency tracking for wireless power transfer systems,” IEEE Trans. Power Electron., vol. 30, no. 7, pp. 4025-4034, Jul. 2015.

[4] D. Ahn, S. Kim, J. Moon, and I. K. Cho, “Wireless power transfer with automatic feedback control of load resistance transformation,” IEEE Trans. Power Electron., vol. 31, no. 11, pp. 7876-7886, Nov. 2016.

[5] M. P. Theodoridis, “Effective capacitive power transfer,” IEEE Trans. Power Electron., vol. 27, no. 12, pp. 4906-4913, Dec. 2012.

[6] D. Thenathayalan, and J. H. Park, “Wide-air-gap transformer model for the design-oriented analysis of contactless power converters,” IEEE Trans. Ind. Electron., vol. 62, no. 10, pp. 6345-6359, Oct. 2015.

[7] M. Fu, Z. Tang, M. Liu, C. Ma, and X. Zhu, “Full-bridge rectifier input reactance compensation in megahertz wireless power transfer systems,” in Proc. 2015 WoW, 2015, pp. 1-5.

[8] A. Berger, M. Agostinelli, S. Vesti, J. A. Oliver, J. A. Cobos, and M. Huemer, “A wireless charging system applying phase-shift and amplitude control to maximize efficiency and extractable power,” IEEE Trans. Power Electron., vol. 30, no. 11, pp. 6338-6348, Nov. 2015.

[9] K. Colak, E. Asa, M. Bojarski, D. Czarkowski, and O. C. Onar, “A novel phase-shift control of semibridgelessactive rectifier for wireless power transfer,” IEEE Trans. Power Electron., vol. 30, no. 11, pp. 6288-6297, Nov. 2015.

[10] Y. Akihara, T. Hirose, S. Masuda, N. Kuroki, M. Numa, and M. Hashimoto, “Analytical study of rectifier circuit for wireless power transfer systems,” in Proc. ISAP, 2016, pp. 338-339.

[11] H. C. Li, K. P. Wang, L. Huang, W. J. Chen, and X. Yang, “Dynamic modeling based on coupled modes for wireless power transfer systems,” IEEE Trans. Power Electron., vol. 30, no. 11, pp. 6245-6253, Nov. 2015.

[12] S. Aldhaher, P. C. K. Luk, K. E. K. Drissi, and J. F. Whidborne, “High-input-voltage high-frequency

class E rectifiers for resonant inductive links," IEEE Trans. Power Electron., vol. 30, no. 3, pp. 1328-1335, Mar. 2015.

[13] H. T. Shi, J. D. Mao, X. S. Li, and J. T. Pan, "Modeling and analysis of impedance for uncontrolled rectifier based nonlinear load," in Proc. CCDC, 2016, pp. 1770-1775.

[14] C. K. Lee, S. Kiratipongvoot, and S. C. Tan, "High-frequency-fed unity power-factor AC-DC power converter with one switching per cycle," IEEE Trans. Power Electron., vol. 30, no. 4, pp. 2148-2156, Apr. 2015.

[15] Q. Lei, M. Shen, V. Blasko, and F. Z. Peng, "A generalized input impedance model of three phase diode rectifier," in Proc. APEC, 2013, pp. 2655-2661.

[16] S. Q. Li, W. H. Li, J. J. Deng, T. D. Nguyen, and C. C. Mi, "A double-sided LCC compensation network and its tuning method for wireless power transfer," IEEE Trans. Veh. Technol., vol. 64, no. 6, pp. 2261-2273, Jun. 2015.

[17] M. Dionigi, M. Mongiardo, and R.Perfetti, "Rigorous network and full-wave electromagnetic modeling ofwireless power transfer links," IEEE Trans. Microwave Theory Tech., vol. 63, no. 1, pp. 65-75, Jan. 2015.

[18] A. Costanzo, M. Dionigi, F. Mastri, M. Mongiardo, G. Monti, J. A. Russer, P. Russer, and L. Tarricone, "Conditions for a load-independent operating regime in resonant inductive WPT," IEEE Trans. Microwave Theory Tech., vol. 65, no. 4, pp. 1066-1076, Apr. 2017.

[19] Q. W. Zhu, L. F. Wang, and C.L. Liao, "Compensate capacitor optimization for kilowatt-level magnetically resonant wireless charging system," IEEE Trans. Ind. Electron., vol. 61, no. 12, pp. 6758-6768, Dec. 2014.

[20] J. W. Kim, D. H. Kim, and Y. J. Park, "Analysis of capacitive impedance matching networks for simultaneous wireless power transfer to multiple devices," IEEE Trans. Ind. Electron., vol. 62, no. 5, pp. 2807-2813, May 2015.

[21] J. Kim, and J. Jeong, "Range-adaptive wireless power transfer using multiloop and tunable matching techniques," IEEE Trans. Ind. Electron., vol. 62, no. 10, pp. 6233-6241, Oct. 2015. [22] W. H. Li, H. Zhao, S. Q. Li, J. J. Deng, T. Z. Kan, and C. C. Mi, "Integrated LCC compensation topology for wireless charger in electric and plug-in electric vehicles," IEEE Trans. Ind. Electron., vol. 62, no. 7, pp. 4215-4225, Jul. 2015.

[23] J. P. W. Chow, H. S. H.Chung, and C. S. Cheng, "Use of transmitter-side electrical information to estimatemutual inductance and regulate receiver-side power in wireless inductive link," IEEE Trans. Power Electron., vol. 31, no. 9, pp. 6079-6091, Sep. 2016.

[24] J. Yin, D. Lin, C. K. Lee, and S. Y. R. Hui, "A systematic approach for load monitoring and power control in wireless power transfer systems without any direct output measurement," IEEE Trans. Power Electron., vol. 30, no. 3, pp. 1657-1667, Mar. 2015

[25] Z. H. Wang, Y. P. Li, Y. Sun, C. S. Tang, and X. Lv, "Load detection model of voltage-fed inductive power transfer system," IEEE Trans. Power Electron., vol. 28, no. 11, pp. 5233-5243, Nov. 2013.

[26] M. F. Fu, H. Yin, X. Zhu, and C. B. Ma, "Analysis and tracking of optimal load in wireless power transfer systems," IEEE Trans. Power Electron., vol. 30, no. 7, pp. 3952-3963, Jul. 2015.

[27] J. Yin, D. Lin, T. Parisini, and S. Y.R. Hui, "Front-end monitoring of the mutual inductance and load resistance in a series-series compensated wireless power transfer system," IEEE Trans. Power Electron., vol. 31, no. 10, pp. 7339-7352, Oct. 2016.

[28] M. Feliziani, T. Campi, S. Cruciani, F. Maradei, U. Grasselli, M. Macellari, and L. Schirone, "Robust LCC compensation in wireless power transfer with variable coupling factor due to coil misalignment," in Proc. 2015 EEEIC, 2015, pp. 1181-1186.

[29] M. Liu, Y. Qiao, and C. B. Ma, "Robust optimization for a 6.78-MHz wireless power transfer system with class E rectifier," in Proc. 2016 WoW, 2016, pp. 88-94.

[30] H. Feng, T. Cai, S. X. Duan, J. B. Zhao, X. M. Zhang, and C. S. Chen, "An LCC-compensated

resonant converter optimized for robust reaction to large coupling variation in dynamic wireless power transfer," IEEE Trans. Ind. Electron., vol. 63, no. 10, pp. 6591-6601, Oct. 2016.

Student Details :

Name: **D. Anna Mani**

Miss D. Anna Mani was graduated from NRIIT, Agiripalli, affliated to Jawaharlal Nehru Technological University, Kakinada. Her special fields of interest include wireless power transfer theory, optimization and control of electric vehicle wireless charging system and bi-directional wireless charging system . Currently she is studying M.Tech in NRI Institute of Engineering, Agiripalli.

Faculty Details:

Name: **Dr. N. Sambasiva Rao**

Dr. N. Sambasiva Rao received the B.Tech degree in Electrical & Electronics Engineering and M. Tech in Electrical Power Engineering from JNTU Hyderabad, India and Ph.D degree from prestigious JNTU Hyderabad India. He has 15 years experience in teaching. He published a 26 research papers in various International Journals and 5 research papers in International ,National Conferences. He got BEST TEACHER AWARD BY JNTU KAKINADA IN THE YEAR 2014. He is the Member of International Association of Engineers (IAENG) and Life member of ISTE. He is currently working as Professor and Head of the department in Electrical & Electronics Engineering at NRI Institute of Technology, Agiripalli, India. He got "Best Achiever award of Andhra Pradesh "By NCERT, New Delhi, India. His Areas of interest include Electrical Machines, FACTS and power System Deregulation.